P6.27

SNOW AND SEA ICE ANGULAR DISTRIBUTION MODEL FROM CERES RADIANCE MEASUREMENTS

Seiji Kato*[1], Norman G. Loeb[1], and Konstantin Loukachine[2]
[1] Center for Atmospheric Sciences
Hampton University, Hampton, Virginia
[2] Science Applications International Corporation
Hampton, Virginia

1. Introduction

Clouds and the Earth's Radiant Energy System (CERES, Wielicki et al. 1996) instruments on Terra are taking measurements of broadband shortwave, longwave and window radiances since March 2000. Because the CERES instruments can be operated under the rotating azimuth mode, they can take radiance measurements over snow covered surface from a wide range of viewing angles. Angular distribution models (ADM) for snow and sea ice are developed in order to estimate top-of-atmosphere broadband shortwave, longwave and window irradiance using measurements by CERES instruments. Because of a large difference of the angular dependence of radiances, ADM is divided into three surface types, permanent snow, fresh snow, and sea ice. ADM scene types are further divided using Moderate Resolution Imaging Spectrometer (MODIS) derived properties (Minnis et al. 2003). This paper briefly describes the method of building empirical shortwave, longwave and window snow angular distribution models that can derive the irradiance from radiance measurements . More detail descriptions are give in Kato et al. (2004). An analysis using the irradiance is also presented in this paper.

2. Shortwave Angular Distribution Model

Footprints that contain snow or sea ice are divided into three surface types, permanent snow, fresh snow, and sea ice, using surface types defined by International Geosphere-Biosphere Programme (IGBP) and National Snow and Ice Data Center (NSIDC, Cavalieri et al. 1990; Comiso 1990) snow and sea ice maps. Because anisotropy of shortwave radiation field is affected by presence of clouds and snow, we use the cloud fraction, snow fraction, cloud optical thickness and snow and sea ice brightness to determine angular distribution model scene types (Table 1).

* Corresponding author address: Seiji Kato, Mail Stop 420, NASA Langley Research Center Hampton, VA 23681-2199; e-mail s.kato@larc.nasa.gov.

Those classification lead to 10 scene types for permanent snow, and 25 scene types for fresh snow and sea ice. To build empirical angular distribution models, we sort the radiance measured by CERES instruments into angular bins. The width of the bin is 5 degree for the viewing zenith angle, 5 degree for the relative azimuth angle and 5 degree for the solar zenith angle (2 degree solar zenith angle for the permanent snow model). We then determine the average radiance $\bar{I}$ and ADM mean irradiance F_{adm} of each scene type. These angular distribution model allow us to estimate the irradiance from each CERES radiance measurement using

$$F = \frac{\pi I}{\langle R \rangle} = \frac{I}{\langle \bar{I} \rangle} \langle F_{adm} \rangle, \tag{1}$$

where I is the instantaneous CERES radiance, R is the anisotropic factor, and $\langle\ \rangle$ indicates the value interpolated at the viewing zenith, relative azimuth, and solar zenith angles of the measurement. Note that $\bar{I}$ and R is a function of scene type in addition to viewing geometry (viewing zenith angle, relative azimuth angle and solar zenith angle).

3. Longwave and Window Angular Distribution Model

Similar to shortwave angular distribution models, longwave models are separated by three surface types. We use the cloud fraction, surface temperature, the surface temperature and cloud effective temperature difference to determine the scene type. These classification lead to 24 scene types for all three surface type angular distribution models. CERES radiances are sorted into viewing zenith angler bins of which width is 2 degree. Therefore, the anisotropic factor of the longwave and window angular distribution model is only a function of viewing zenith angle and scene type. Daytime and nighttime models are built from daytime and nighttime data, respectively, using the same scene type classification.

4. Consistency Check Using CERES Along-Track Data

As a part of a consistency check of estimated irradiances, we apply the angular distribution models to CERES along-track data and derive the irradiance from different viewing zenith angles for the same scene. If we select a uniform object, the irradiance should be nearly constant with viewing zenith angle (Loeb et al. 2003). Figure 1 shows CERES radiances I and the average radiance $\bar{I}$ from angular distribution model used to derive the irradiance for two selected scenes. Because the irradiance is derived by scaling the ADM mean irradiance by the ratio of the CERES radiance to the average radiance, the derived irradiances are nearly constant with viewing zenith angle when the shape of $\bar{I}$ as a function of viewing angle is similar to the observed shape of I. The variation of the irradiance with viewing angle, which is caused by variations of surface and cloud properties and angular distribution model error, is within 10% for the shortwave case and within 3% for the longwave case. A study by Kato et al. (2004) suggests that the bias error in the shortwave irradiance is less than 1% and regional root mean square error is less than 6%.

Table 1: Snow and Sea Ice Shortwave Angular Distribution Model Scene Types

Cloud Fraction	Snow and Sea Ice Fraction	Cloud Optical Thickness	Snow Brightness
Permanent Snow			
$\leq$ 0.001	-	≤ 10	Dark
0.01 - 0.25		> 10	Bright
0.25 - 0.50			
0.50 - 0.75			
0.75 - 0.999			
$>$ 0.999			
Fresh Snow and Sea Ice			
$\leq$ 0.01	$\leq$ 0.01	≤ 10	Dark
0.01 - 0.25	0.01 - 0.25	> 10	Bright
0.25 - 0.50	0.25 - 0.50		
0.50 - 0.75	0.50 - 0.75		
0.75 - 0.999	0.75 - 0.999		
$>$ 0.99	$>$ 0.99		

5. Net Radiation over Sea Ice

Figure 2 shows the top-of-atmosphere albedo, top-of-atmosphere upward longwave irradiance (OLR), and top-of-atmosphere net radiation estimated over sea ice surfaces as a function of the solar zenith angle and surface temperature. Both the albedo and OLR is a strong function of surface temperature. The reason for the albedo being a function of the solar zenith angle is shown in Figure 3. The albedo decreases with increasing solar zenith angle because sea ice melts as the solar zenith angle increases. A part of the reason for a large sea ice fraction at the surface temperature above 273 K is that only CERES footprints that contains sea ice (sea ice fraction is greater than 0) are used for this analysis. Therefore, 45% sea ice faction at the surface temperature above 273 K does not mean the 45% of the time sea ice is present at the surface temperature above freezing. Figure 3 also shows that the clear fraction decreases and cloud optical thickness increases with increasing surface temperature. Net radiation is primarily a function of the solar zenith angle but the contour is slightly tilted when the surface temperature is larger than $\approx$ 273K. The contour indicates that the when surface temperature is perturbed to a slightly higher temperature, the atmospheric and surface properties changes so that the net radiation is more positive (more energy absorbed by the earth system) if the surface temperature is above $\approx$ 273K. When the surface temperature is less than 270 K and the solar zenith angle is greater than 70°, Figure 2 also indicates that the net radiation decreases if the surface temperature is perturbed to a slightly higher temperature.

Table 2: Snow and Sea Ice Longwave and Window Angular Distribution Model Scene Types

Cloud Fraction	Surface Temperature Fraction	Cloud Top Surface Temperature Difference
$\leq$ 0.001	$<$ 250 K	$<$ 20 K
0.01 - 0.25	$\geq$ 250 K	$\geq$ 20 K
0.25 - 0.50	(Parm. Snow	
0.50 - 0.75	Night	
0.75 - 0.999	$<$ 240 K	
$>$ 0.999	$\geq$ 240 K)	

6. Summary

Snow and sea ice angular distribution models are developed to estimate the irradiance from radiance measurements. Collocation of imager radiances, which are used for scene identifications, allow us to build scene type dependent angular distribution models. Because of these scene type dependent angular distribution models, the error in the irradiance does not significantly increases when the radiance is averaged over a region for for a specific atmospheric or surface conditions. Therefore, analyses of top-of-atmosphere

radiation as a function of sea ice fraction or cloud fraction over polar regions can be done with CERES data set.

Acknowledgments

We thank B. A. Wielicki for useful discussions. The work is supported by the Clouds and the Earth's Radiant Energy System (CERES) project under NASA grant (NNL04AA26G).

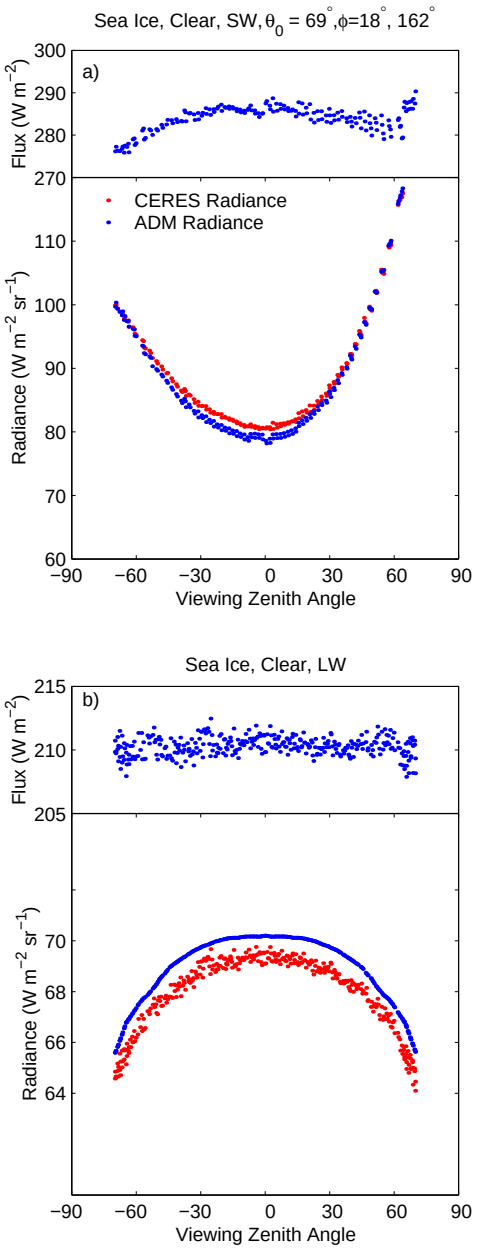

Figure 1 The irradiance derived by a) Permanent snow and b) sea ice angular distribution models using along-track data over uniform scenes.

References

Cavalieri, D., P. Gloerson, and J. Zwally; DMSP SSM/I daily polar gridded sea ice concentrations. Edited by J. Maslanik and J. Stroeve. Boulder, CO: National Snow and Ice Data Center. Digital media, 1990.

Comiso, J.; DMSP SSM/I daily polar gridded sea ice concentrations. Edited by J. Maslanik and J. Stroeve. Boulder, CO: National Snow and Ice Data Center. Digital media, 1990.

Kato, S., and N. G. Loeb, 2004: Top-of-atmosphere shortwave broadband observed radiance and estimated irradiance over polar regions from Clouds and the Earth's Radiant Energy System (CERES) instruments on Terra, Submitted to *J. Geophys. Res.*

Loeb, N. G., K. Loukachine, N. M. Smith, B. A. Wielicki and D. F. Young; Angular distribution models for top-of-atmosphere radiative flux estimation from the clouds and the Earth's radiant energy system instrument of the tropical rainfall measuring mission satellite. Part II: Validation *J. Appl. Meteor.*, **42**, 1748-1769, 2003.

Minnis, P., D. F. Young, S. Sun-Mack, P. W. Heck, D. R. Doelling, and Q. Trepte: CERES Cloud Property Retrievals from Imagers on TRMM, Terra, and Aqua, *Proc. SPIE 10th International Symposium on Remote Sensing*, Conference on Remote Sensing of Clouds and the Atmosphere VII, Barcelona, Spain, September 8-12, 37-48, 2003.

Wielicki, B. A., B. R. Barkstrom, E. F. Harrison, B. B. Lee III, G. Louis Smith, and J. E. Cooper: Clouds and the Earth's radiant energy system (CERES); an earth observing system experiment, *Bull. Amer. Meteor. Soc.*, **77**, 853-868, 1996

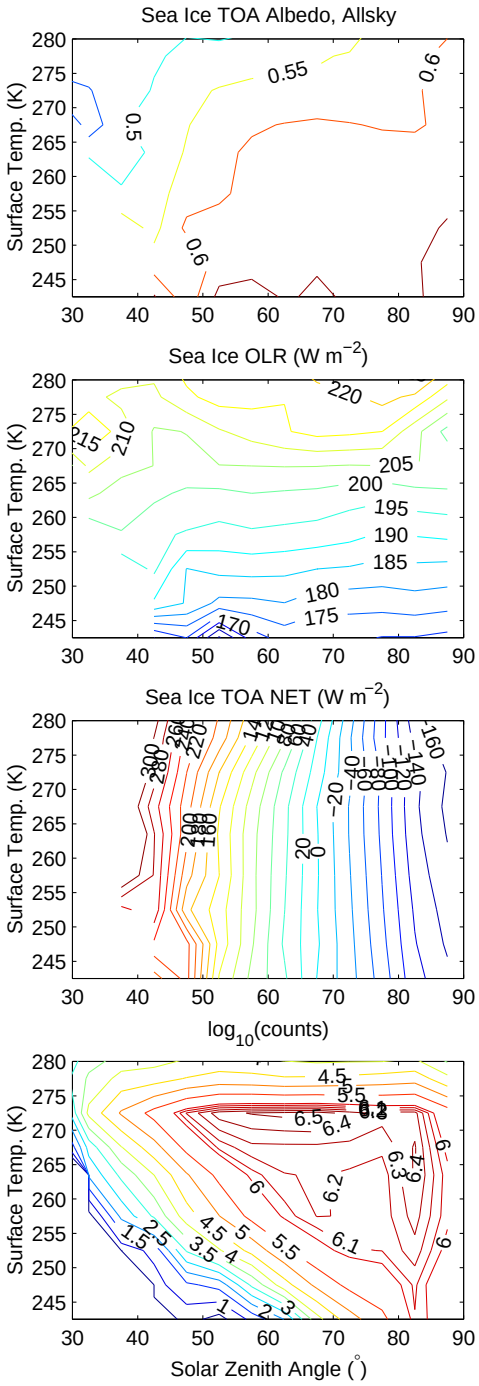

Figure 2 Top-of-atmosphere albedo, upward longwave irradiance, net radiation (positive when energy is deposited to the earth system), and logarithmic of the number of samples in each bin. These are estimated from CERES measurements taken over sea ice surface.

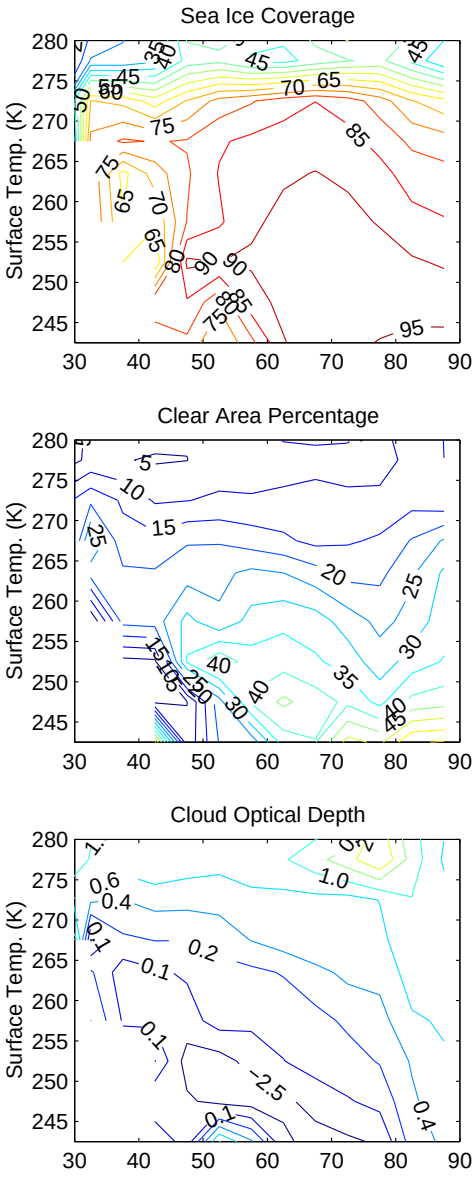

Figure 3 Sea ice coverage, clear area percentage (100% - cloud cover), and cloud optical depth over CERES footprints as a function of solar zenith angle and surface temperature.